



Anti-Reflection Property of SiO₂ Composite Films for Solar Cell

H. Nagehan Koysuren & Ozcan Koysuren

To cite this article: H. Nagehan Koysuren & Ozcan Koysuren (2026) Anti-Reflection Property of SiO₂ Composite Films for Solar Cell, Journal of Macromolecular Science, Part B, 65:2, 250-260, DOI: [10.1080/00222348.2024.2414582](https://doi.org/10.1080/00222348.2024.2414582)

To link to this article: <https://doi.org/10.1080/00222348.2024.2414582>



Published online: 13 Oct 2024.



Submit your article to this journal [↗](#)



Article views: 134



View related articles [↗](#)



View Crossmark data [↗](#)



Citing articles: 3 View citing articles [↗](#)



Anti-Reflection Property of SiO₂ Composite Films for Solar Cell

H. Nagehan Koysuren^a and Ozcan Koysuren^b

^aDepartment of Environmental Engineering, Ahi Evran University, Kirsehir, Turkey; ^bDepartment of Energy Engineering, Ankara University, Ankara, Turkey

ABSTRACT

In this study, anti-reflection property of SiO₂ based composite films were investigated. For this purpose, SiO₂/TiO₂, SiO₂/ZnO and SiO₂/TiO₂/ZnO composite films were prepared using a sol-gel technique and coated on glass slides. Polyethylene glycol (PEG) with molecular weight of 1500 g/mol was inserted into the SiO₂ composite film as a porogen to decrease the refractive index and improve the anti-reflection property of the as-prepared film. The SiO₂ films with pore structures were successfully obtained. The PEG modified SiO₂/ZnO (SiO₂/PEG/ZnO) film provided a water contact angle close to the water contact angle of a superhydrophilic surface. In addition, the SiO₂/PEG/ZnO film exhibited the highest average transmittance of 92.7% higher than that of the uncoated glass slide. The photovoltaic conversion efficiency of the solar cell coated with the SiO₂/PEG/ZnO film was very close to that of the solar cell without the film coating. Hence, the results exhibited that the SiO₂/PEG/ZnO film with anti-reflection and photovoltaic conversion efficiency has a potential application on solar cells.

ARTICLE HISTORY

Received 23 September 2024
Accepted 2 October 2024

KEYWORDS

SiO₂; ZnO; PEG; TiO₂; anti-reflection coating; solar cell

1. Introduction

Photovoltaic (PV) energy has become an attractive source of renewable energy because of the minimal environmental impact of PV energy production and the abundance of solar energy. An important phenomenon reducing the power conversion efficiency of PV devices is the surface reflection, which occurs due to the refractive index contrast between the solar cell and air.^[1] The surface reflection has been a major problem in the solar cell industry since an unmodified solar cell (silicon-based) can exhibit more than 30% reflection, leading to low short circuit currents. Several approaches, like anti-reflection coating or surface texturing, have been applied to reduce the light reflection of the silicon solar cell.^[2] Anti-reflective (AR) coatings are an important application to reduce the surface reflection losses and thus increase the solar cell efficiency.^[1]

As an anti-reflection coating, nanostructured arrays, multilayer interference coatings, thin-film (quarter-wavelength) coatings and gradient refractive index coatings have been applied to reduce the surface reflection losses. Compared to the specified coatings, the

CONTACT H. Nagehan Koysuren  nagehan.koysuren@ahievran.edu.tr  Department of Environmental Engineering, Ahi Evran University, Kirsehir, Turkey; Ozcan Koysuren  koysuren@ankara.edu.tr  Department of Energy Engineering, Ankara University, Ankara, Turkey.

preparation of thin film (quarter-wavelength coatings) is simpler and cheaper.^[3] The most suitable thin-film materials are silica with the refractive (n) of 1.44, magnesium fluoride ($n = 1.35$), titanium dioxide ($n = 2.2$) and alumina ($n = 1.65$). These coatings also possess excellent adhesion strength and abrasion resistance.^[4] In order to prevent the surface reflection on the cover glass of the solar cells with refractive index of 1.44, the thin film coating should have a refractive index of 1.21. Since there is no material with this refractive index, we suggest nano-porous surface structure might be obtained in the thin film coatings to reduce its refractive index.^[3]

To prepare thin-film coatings based on silica with low surface reflection, porogens can be added into the silica film. The porogens are easily degradable macromolecules and added into the silica solution before the film coating process. Uniform nano-pores can be formed in the silica coating after removing the porogens through the heat treatment process. In the literature, different types of the porogens, such as polyethylene glycol (PEG)^[5], polyvinyl pyrrolidone (PVP)^[6], poly(ethylene oxide)-*b*-poly(propylene oxide)-*b*-poly(ethylene oxide) (PEO105-PPO70-PEO105)^[7], polypropylene glycol (PPG)^[4] and polyethylene glycol tercoctylphenyleter (Triton X-100)^[8], have been combined with the silica coating to form nano-pores on its surface. The silica coatings with nano-pore structure maintain their high abrasion-resistance, while at the same time gaining low refractive index.^[4] According to the study of Li and his coworkers,^[6] for instance, high light transmittance was achieved with the silica coating having a PEG-derived nanopore structure. The solar cell efficiency of the copper indium gallium selenide (CIGS) solar cell coated with an SiO₂-PEG film increased by 7.27%.^[6] Similarly, Wongcharee and his coworkers (2002) obtained an average transmittance of 98.6% for a SiO₂-PEG coated glass slide over the visible region.^[9] The average transmittance value (95.5%) of an SiO₂-PEG coated glass substrate increased by 5.5% over the average value of the uncoated glass substrate in the study by Dou and his coworkers.^[10] The pore formation ability of PEG is primarily proportional to its molecular weight. According to the study by Dou and his coworkers,^[10] PEG with a molecular weight of 4000 g/mol resulted in higher porosity and higher transmittance than PEG with a molecular weight of 1000 g/mol.^[10]

On the other hand, there are several techniques to prepare thin-film coatings. Among the techniques, the sputtering technique has been used to coat thin layers on substrates with different shapes. This technique has been applied for the deposition of anti-reflection coatings on display devices and thermochromic windows. Similarly, the chemical vapor deposition technique and the physical vapor deposition technique have been utilized to prepare coatings with controlled refractive indices and thicknesses. However, these specified coating techniques have substrate size limitation and require a moderate vacuum for deposition, which limits the spread of the technology into wider applications. Compared to the above specified coating techniques, the sol-gel techniques have the advantages of low cost and simple process. The sol-gel techniques can be applied to substrates with different sizes and shapes. In addition, the surface structure can be controlled, which allows to adjust the refractive index of the coating.^[11]

In order to increase the durability of the SiO₂ thin film coating in outdoor conditions, it can be combined with TiO₂, ZnO and similar semiconductors within the film structure.^[12,13] Nano-porous SiO₂/TiO₂ or SiO₂/ZnO composite films might be a good

candidate for the top layer of the solar cell. The presence of TiO_2 or ZnO in the film coating can enhance the mechanical properties and control the optical properties.^[12,13] Both ZnO and TiO_2 , depending on the particle size, can exhibit high light transmission in the visible light range. They can absorb mostly short wavelength UV light. However, ZnO and TiO_2 have slightly higher refractive indices compared to SiO_2 . The presence of TiO_2 or ZnO in the SiO_2 coating would increase the refractive index of the resulting film.^[12,13] Therefore, the TiO_2 or ZnO content of the composite content should be limited.

The performance of solar cells is significantly reduced by dust and organic contaminants that accumulate on the cover glass. Accumulated contaminants on the cover glass of the solar cell can reduce the photoelectric conversion efficiency by reflecting and/or absorbing the incoming light. TiO_2 ,^[14] ZnO ,^[14] B_4C ,^[15] SnO_2 ,^[16] and CuO ^[17] are known as effective self-cleaning materials for solar cells due to their superior stability, excellent photocatalytic behavior and superhydrophilic structure. All these semiconductor materials have numerous reactive sites that enhance the hydrophilic behavior under sunlight. The hydrophilic behavior of these semiconductor materials is important for self-cleaning applications.^[14–17] Self-cleaning surfaces allow water droplets to roll off the surface on contact, collecting and removing dust and other contaminants.

In this manuscript, an effective approach to enhance the solar cell efficiency by using SiO_2 based anti-reflection coatings to reduce the surface reflection losses of the solar cell is reported. Polyethylene glycol (PEG), as a porogen, was added into the silica solution. In addition, TiO_2 and/or ZnO nanoparticles were added into the SiO_2 solution to prepare $\text{SiO}_2/\text{PEG}/\text{TiO}_2$, $\text{SiO}_2/\text{PEG}/\text{ZnO}$ and $\text{SiO}_2/\text{PEG}/\text{TiO}_2/\text{ZnO}$ coatings. The TiO_2 and/or ZnO nanoparticles were added into the SiO_2 thin film to enhance the hydrophilic behavior of the resulting coating. The anti-reflection performance of the as-prepared composite coatings was investigated. In addition, the effect of the composite coating on the solar cell efficiency was studied. We note that the SiO_2 is an important example of a macromolecular solid, which means that SiO_2 is highly cross-linked, forming thousands of covalent bonds between its silicon and oxygen atoms. Physical properties (morphology, water contact angle, refractive index), optical properties (UV-Vis absorbance, transmittance) and photoelectric properties (solar cell efficiency) of the SiO_2 composite films were investigated within this manuscript.

2. Experimental

2.1. Preparation of SiO_2 composite films

SiO_2 solutions were prepared using the acid catalyzed technique to coat glass slides with the SiO_2 composite films.^[5] Firstly, 112 ml of tetraethylorthoxylsilicane (TEOS) was mixed with a water-anhydrous ethanol solution (36 ml-1090 ml). Then, 0.2 ml of hydrochloric acid solution (36%) was added into the as-prepared solution. Then, polyethylene glycol (PEG), with a molecular weight of 1500 g/mol, was added into the TEOS solution at the PEG to TEOS mass ratio of 0.5 under constant stirring, followed by adding TiO_2 and/or ZnO nanoparticles into the SiO_2/PEG solution under stirring for 1 day. The TiO_2 and/or ZnO content of the final SiO_2 film was adjusted to be 10 wt.%. The SiO_2 solution, including TiO_2 and/or ZnO nanoparticles, was dip-coated on both sides of

glass slides and then the glass slides were oven-dried at 100 °C for 1 h. Finally, they were exposed to heat treatment at 550 °C for 1 h.^[5] The final SiO₂ film, including TiO₂, ZnO or TiO₂/ZnO, were labeled as SiO₂/PEG/TiO₂, SiO₂/PEG/ZnO and SiO₂/PEG/TiO₂/ZnO, respectively.

2.2. Methods of characterization

To investigate the surface morphology of the SiO₂ composite films, optical microscopy images were obtained on a binocular microscope (DMS-633, Leica Microsystems GmbH, Germany). The UV-Vis absorbance spectrum and transmittance spectrum of the SiO₂ composite films were obtained by using a spectrophotometer (Genesys 10S, Thermo Fisher Scientific Inc., USA) both in the absorbance mode and transmittance mode. The photoelectric conversion efficiency of solar cells coated with the SiO₂ composite films was recorded by using a solar module analyzer (PROVA 210, Prova Instruments Inc., Taiwan). The water contact angle measurement of the SiO₂ composite films was performed by using a Theta Lite model optical tensiometer (Biolin Scientific AB, Sweden).

3. Results and discussion

3.1. Morphology analysis

Figure 1 illustrates the optical microscopy image of the SiO₂ composite film samples. A homogeneous coating structure could not be obtained with the SiO₂/PEG/TiO₂ film. A lot of crack structures were observed on the image of the SiO₂/PEG/TiO₂ film (Figure 1a). No crack structures were observed on the image of the SiO₂/PEG/ZnO film (Figure 1b). In addition, very small crack structures were observed on the optical microscopy of SiO₂/PEG/TiO₂/ZnO film (Figure 1c). The cracks might occur during the drying step of the film coating process due to the removal of solvent. The dark spherical regions in the SiO₂/PEG/TiO₂, SiO₂/PEG/ZnO and SiO₂/PEG/TiO₂/ZnO film might belong to the TiO₂ and/or ZnO nanoparticles in agglomerate structure. The optical microscopy image of the SiO₂/PEG/TiO₂ film exhibited various particle sizes of the TiO₂ agglomerates in the SiO₂ phase. On the other hand, the optical microscopy images of the SiO₂/PEG/ZnO and SiO₂/PEG/TiO₂/ZnO film revealed smaller agglomerate size



Figure 1. Optical microscopy images of (a) SiO₂/PEG/TiO₂, (b) SiO₂/PEG/ZnO and (c) SiO₂/PEG/TiO₂/ZnO films.

of the ZnO nanoparticles in the SiO₂ phase. The PEG molecules used as porogens might be successfully removed during the heat treatment step of the film coating process, which enabled the formation of the pore structures in SiO₂ composite films. However, the specified pore structures could be noticed on the optical microscope images of the film samples.

3.2. UV-Vis absorption study

The UV-Vis absorption spectrum of the film samples is presented in Figure 2. The spectra indicated that all film samples mostly absorbed light in the UV region at around 300 nm. None of the composite film samples showed light absorption in the visible wavelength region. Hence, the film samples could be a suitable candidate as an anti-reflection coating on solar cells under natural sunlight. The Tauc's relation (1) was followed to calculate the optical band gap energy of the as-prepared film samples:^[18]

$$(\alpha h\nu)^2 = A(h\nu - E_g) \quad (1)$$

where $h\nu$ is the photon energy, α is the absorption coefficient, A is a constant and E_g is the optical band gap energy, respectively. Figure 3 illustrates the absorbance spectrum of the film samples. The region of the $(\alpha h\nu)^2$ vs. $(h\nu)$ curve showing that the light absorption increased steeply and linearly with increasing the photon energy is characteristic of semiconductor materials. The x-axis intersection point of the linear part of the $(\alpha h\nu)^2$ vs. $(h\nu)$ curve gives an estimate of the optical band gap energy.^[18] The optical band gap energies for SiO₂/PEG/TiO₂, SiO₂/PEG/ZnO and SiO₂/PEG/TiO₂/ZnO were estimated to be 4.10 eV, 4.20 eV and 4.15 eV, respectively. Thus, according to the results, all the film samples exhibited similar optical band gap values.

3.3. Light transmittance study

Figure 4 illustrates the transmittance spectra of the film samples. The average transmittance of the SiO₂/PEG/ZnO film in the wavelength range of 358-800 nm was about 92.6%. Compared with the average transmittance of the uncoated glass slide (reference)

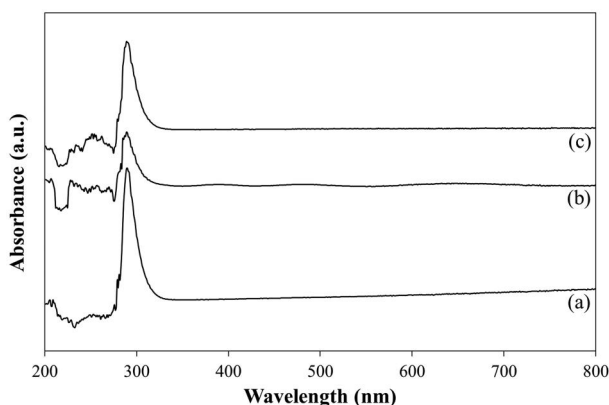


Figure 2. UV-Vis absorbance spectrum of (a) SiO₂/PEG/TiO₂, (b) SiO₂/PEG/ZnO and (c) SiO₂/PEG/TiO₂/ZnO films.

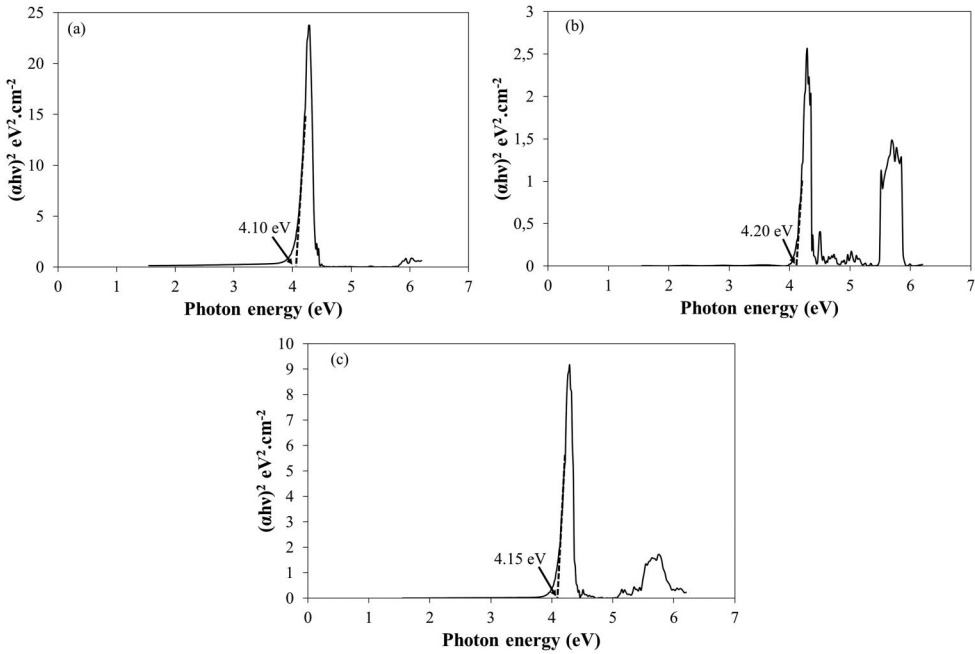


Figure 3. Tauc's plot for (a) $\text{SiO}_2/\text{PEG}/\text{TiO}_2$, (b) $\text{SiO}_2/\text{PEG}/\text{ZnO}$ and (c) $\text{SiO}_2/\text{PEG}/\text{TiO}_2/\text{ZnO}$ films.

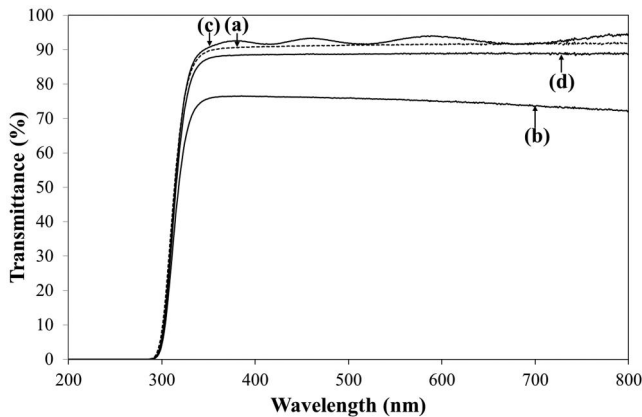


Figure 4. Light transmittance spectrum of (a) uncoated glass slide, (b) $\text{SiO}_2/\text{PEG}/\text{TiO}_2$, (c) $\text{SiO}_2/\text{PEG}/\text{ZnO}$ and (d) $\text{SiO}_2/\text{PEG}/\text{TiO}_2/\text{ZnO}$ films.

of about 91.4%, an improvement of more than 1% in light transmittance was achieved. For the $\text{SiO}_2/\text{PEG}/\text{TiO}_2$ film, the average transmittance obtained was about 74.9%, decreasing about 16% compared with that of the uncoated glass slide. The average transmittance of the $\text{SiO}_2/\text{PEG}/\text{TiO}_2/\text{ZnO}$ film in the wavelength range of 358–800 nm was about 88.7%, decreasing about 3% compared with that of the uncoated glass slide. The transmittance thus tended to decrease after coating the glass slide with the SiO_2 film including the TiO_2 phase. This loss of transmittance might be due to the increased refractive index caused by TiO_2 , which reduced the portion of incident light entering the film.

The thickness of the film samples was calculated by using the transmittance spectrum of the film samples through the following relation:^[19]

$$d = 1/n (\lambda/4 (2m + 1)) \quad (2)$$

where d is the film thickness, n is the refractive index and m is the order of the minimum transmittance ($T_{\min \text{ abs}}$) in the high transmittance region ($m=1$ for the $\text{SiO}_2/\text{PEG}/\text{TiO}_2$ and $\text{SiO}_2/\text{PEG}/\text{TiO}_2/\text{ZnO}$ films, $m=3$ for the $\text{SiO}_2/\text{PEG}/\text{ZnO}$ film). On the other hand, the refractive index (n) at the absolute minimum transmittance ($T_{\min \text{ abs}}$) was calculated using the following relation:^[19]

$$n = \left((n_0 n_2)^{0.5} (1 + (1 - T_{\min \text{ abs}})^{0.5}) / (T_{\min \text{ abs}})^{0.5} \right) \quad (3)$$

at which n_0 ($n_0=1$) and n_2 ($n_2=1.515$) are the refractive indices of air and the glass slide, respectively. The film thickness and refractive index values of the film samples are shown in Table 1. The calculated thicknesses for the $\text{SiO}_2/\text{PEG}/\text{TiO}_2$, $\text{SiO}_2/\text{PEG}/\text{ZnO}$ and $\text{SiO}_2/\text{PEG}/\text{TiO}_2/\text{ZnO}$ film samples were 127.5 nm, 434.7 nm and 159.6 nm, respectively. While similar film thicknesses were obtained with the $\text{SiO}_2/\text{PEG}/\text{TiO}_2$ and $\text{SiO}_2/\text{PEG}/\text{TiO}_2/\text{ZnO}$ samples, a thicker film thickness was obtained with the $\text{SiO}_2/\text{PEG}/\text{ZnO}$ sample. It was understood that the ZnO phase significantly affected the film thickness. The refractive index of the $\text{SiO}_2/\text{PEG}/\text{TiO}_2$ film measured at $\lambda = 359$ nm was 2.11 and the refractive index of the $\text{SiO}_2/\text{PEG}/\text{ZnO}$ film measured at $\lambda = 412$ nm was 1.66. In general, the refractive index of the SiO_2 film increased with the contribution of the semiconductor nanoparticles, which might be due the size and filling effects of the nanoparticles.^[17] TiO_2 nanoparticles might lead to the formation of a dense composite film, reducing the porosity and thus increasing the refractive index.^[20] The refractive index of the $\text{SiO}_2/\text{PEG}/\text{TiO}_2/\text{ZnO}$ film measured at $\lambda = 374$ nm was 1.76, close to that of the $\text{SiO}_2/\text{PEG}/\text{ZnO}$ film. A film with a porous film structure has a lower refractive index than a film with less porosity.^[21] According to the low refractive index values of the films containing ZnO, it could be concluded that the films containing the ZnO phase were more porous or less dense.

3.4. Water contact angle measurement

The water contact angle measurement is an important characterization technique to observe the wettability of a surface. It is generally accepted that the surface has a self-cleaning property when the water contact angle is less than 5° or more than 150° . If the water contact angle on the surface is less than 5° , the surface is known as superhydrophilic.^[22] According to Figure 5, the water contact angles of the $\text{SiO}_2/\text{PEG}/\text{TiO}_2$, $\text{SiO}_2/\text{PEG}/\text{ZnO}$ and $\text{SiO}_2/\text{PEG}/\text{TiO}_2/\text{ZnO}$ film samples were found to be 29.09° , 14.15° and 16.71° , respectively. Among the prepared film samples, the $\text{SiO}_2/\text{PEG}/\text{ZnO}$ film sample

Table 1. The refractive index (n) at the absolute minimum transmittance in the high transmittance region and the film thickness value of the SiO_2 composite films.

Sample	λ (nm) at $T_{\min \text{ abs}}$	$T_{\min \text{ abs}}$	n	d (nm)
$\text{SiO}_2/\text{PEG}/\text{TiO}_2$	359	0.757	2.11	127.5
$\text{SiO}_2/\text{PEG}/\text{ZnO}$	412	0.916	1.66	434.7
$\text{SiO}_2/\text{PEG}/\text{TiO}_2/\text{ZnO}$	374	0.883	1.76	159.6

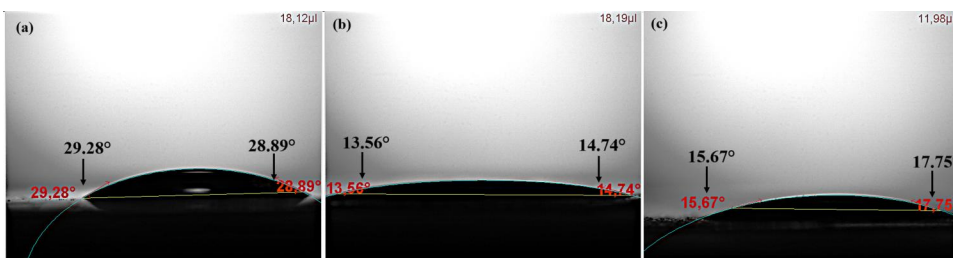


Figure 5. The water contact angle of (a) SiO₂/PEG/TiO₂, (b) SiO₂/PEG/ZnO and (c) SiO₂/PEG/TiO₂/ZnO films.

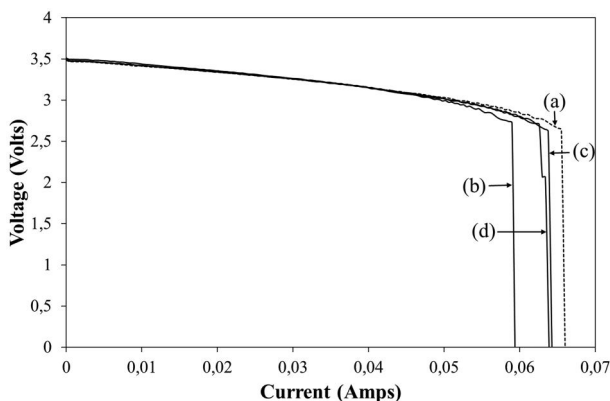


Figure 6. Current-voltage (I-V) characteristics of (a) the standard solar cell and the solar cell coated with (b) SiO₂/PEG/TiO₂, (c) SiO₂/PEG/ZnO, (d) SiO₂/PEG/TiO₂/ZnO films.

showed the highest hydrophilic property, enabling the coating to improve its self-cleaning performance. During the heat treatment of the film samples, PEG molecules might be removed, which could cause nanopores to form on the film surface and increase the roughness of the film. This might be the reason for the low water contact angle on the SiO₂ composite film samples. The superhydrophilic property of an anti-reflective film enables the coating surface to self-clean, thus eliminating the influence of dust or other contaminants on the light transmittance.^[22]

3.5. Photovoltaic conversion efficiency

To study the effect of the SiO₂ composite film samples on the photovoltaic conversion performance of the solar cells, I-V measurements were performed. According to the I-V measurements (Figure 6), the fill factor (FF) and the photoelectric conversion efficiency (η) were calculated using the following relations:^[23]

$$FF = \frac{V_{MP}I_{MP}}{V_{OC}I_{SC}} \tag{4}$$

$$\eta \text{ (efficiency)} = \frac{V_{OC}I_{SC}FF}{P_{in}} \tag{5}$$

where V_{MP} and I_{MP} are the voltage at the maximum power point and the current at the maximum power point, respectively, V_{OC} is the open circuit voltage, I_{SC} is the short circuit current and P_{in} is the incident power.^[23] The fill factor has been known as one of

Table 2. The photoelectric conversion efficiency of the standard solar cell and the solar cell coated with the SiO₂ composite films.

Sample	V _{MP} (V)	I _{MP} (A)	V _{oc}	I _{sc}	FF	A (m ²)	P _{out} (W/m ²)	P _{in} (W/m ²)	η _c (%)
Standard	2.757	0.0633	3.487	0.066	0.758	0.0016	109.1	1170	9.32
SiO ₂ /PEG/TiO ₂	2.726	0.0590	3.511	0.059	0.776	0.0016	100.5	1170	8.59
SiO ₂ /PEG/ZnO	2.772	0.0612	3.494	0.064	0.759	0.0016	106.0	1170	9.06
SiO ₂ /PEG/TiO ₂ /ZnO	2.705	0.0626	3.493	0.064	0.757	0.0016	105.8	1170	9.04

the key electrical parameters quantifying the photoelectric conversion performance of solar cells. The fill factor is directly proportional to the photoelectric power conversion efficiency. That is, higher fill factor leads to higher solar cell efficiency.^[24] Among the solar cells coated with the SiO₂ composite films, only the solar cell coated with the SiO₂/PEG/TiO₂/ZnO film had a slightly lower FF value than the standard solar cell (Table 2). The fill factor results revealed that the SiO₂ composite films can be coated on the upper glass cover of the real photovoltaic system and improve their efficiency. The photoelectric conversion efficiency of the standard uncoated solar cell was calculated to be 9.32%. On the other hand, the efficiency of the solar cell coated with the SiO₂/PEG/TiO₂, SiO₂/PEG/ZnO and SiO₂/PEG/TiO₂/ZnO film were calculated to be 8.59%, 9.06% and 9.04%, respectively. When compared with the standard solar cell, slightly lower efficiencies were obtained with the solar cell coated with the SiO₂/PEG/ZnO and SiO₂/PEG/TiO₂/ZnO films, respectively. The accumulation of dust or other contaminants on the surface of a solar cell forms a barrier, preventing the incoming sunlight from reaching the absorber layer and thus reducing its photovoltaic conversion efficiency in time.^[25] The self-cleaning feature of the SiO₂ composite films with low water contact angles can prevent the decrease in the photovoltaic conversion efficiency. Although initially slightly less efficient than the uncoated solar cell, the SiO₂ film-coated solar cells are expected to become more advantageous in terms of their photovoltaic conversion efficiency over time due to their self-cleaning feature.

4. Conclusions

In this study, glass slides were coated with SiO₂ composite films to obtain anti-reflection coatings for solar cells by the dip-coating process. The SiO₂ composite film with ZnO nanoparticles showed higher transmittance compared to the uncoated glass slides. PEG molecules were used as a porogen to induce the formation of pore structures on the film surface, which could result in lower refractive index and higher transmittance with the composite films. In addition, the SiO₂ composite film including the ZnO nanoparticles provided low water contact angles. The hydrophilic feature of the composite film could also provide self-cleaning properties. The current-voltage measurement of the solar cell coated with the SiO₂ composite films did not exhibit any significant loss in the photoelectric conversion efficiency, suggesting that the SiO₂ composite films can be applied as an anti-reflective coating on commercial solar cell systems.

Disclosure statement

No potential conflict of interest was reported by the author(s).

Funding

The authors declare that no funds, grants, or other support were received during the preparation of this manuscript. The budget required for the experimental studies was covered by the salaries of the authors.

References

- [1] Yan, X.; Poxson, D. J.; Cho, J.; Welser, R. E.; Sood, A. K.; Kim, J. K.; Schubert, E. F. Enhanced Omnidirectional Photovoltaic Performance of Solar Cells Using Multiple-Discrete-Layer Tailored-and Low-Refractive Index anti-Reflection Coatings. *Adv. Funct. Materials* **2013**, *23*, 583–590. DOI: [10.1002/adfm.201201032](https://doi.org/10.1002/adfm.201201032).
- [2] Valiei, M.; Shaibani, P. M.; Abdizadeh, H.; Kolahdouz, M.; Soleimani, E. A.; Poursafar, J. Design and Optimization of Single, Double and Multilayer anti-Reflection Coatings on Planar and Textured Surface of Silicon Solar Cells. *Mater. Today Commun.* **2022**, *32*, 104144. DOI: [10.1016/j.mtcomm.2022.104144](https://doi.org/10.1016/j.mtcomm.2022.104144).
- [3] Zhang, L.; Wei, H.; Ren, L.; Wang, P.; Hu, Z.; Shang, J.; Zhou, J. Antireflective Coatings of Chitin Nanofibers on Glass Fabricated through Electric Field Deposition. *Mater. Today Commun.* **2023**, *37*, 107442. DOI: [10.1016/j.mtcomm.2023.107442](https://doi.org/10.1016/j.mtcomm.2023.107442).
- [4] Xia, B.; Zhang, Q.; Yao, S.; Zhang, Y.; Xiao, B.; Jiang, B. Sol-Gel Silica Antireflective Coating with Enhanced Abrasion-Resistance Using Polypropylene Glycol as Porogen. *J. Sol-Gel Sci. Technol.* **2014**, *71*, 291–296. DOI: [10.1007/s10971-014-3362-0](https://doi.org/10.1007/s10971-014-3362-0).
- [5] Zhu, Y.; Chen, L.; Zhang, C.; Guan, Z. Preparation of Hydrophobic Antireflective SiO₂ Coating with Deposition of PDMS from Water-Based SiO₂-PEG Sol. *Appl. Surf. Sci.* **2018**, *457*, 522–528. DOI: [10.1016/j.apsusc.2018.06.177](https://doi.org/10.1016/j.apsusc.2018.06.177).
- [6] Li, D.; Liu, Z.; Wang, Y.; Shan, Y.; Huang, F. Efficiency Enhancement of Cu(In,Ga)Se₂ Solar Cells by Applying SiO₂-PEG/PVP Antireflection Coatings. *J. Mater. Sci. Technol.* **2015**, *31*, 229–234. DOI: [10.1016/j.jmst.2014.11.003](https://doi.org/10.1016/j.jmst.2014.11.003).
- [7] Chi, F.; Yan, L.; Lv, H.; Jiang, B. Novel Pathways for the Preparation of Silica Antireflective Films: Improvement in Mechanical Property. *Mater. Lett.* **2011**, *65*, 1095–1097. DOI: [10.1016/j.matlet.2011.01.025](https://doi.org/10.1016/j.matlet.2011.01.025).
- [8] Bautista, M. C.; Morales, A. Silica Antireflective Films on Glass Produced by the Sol-Gel Method. *Sol. Energy Mater. Sol. Cells* **2003**, *80*, 217–225. DOI: [10.1016/j.solmat.2003.06.004](https://doi.org/10.1016/j.solmat.2003.06.004).
- [9] Wongcharee, K.; Brungs, M.; Chaplin, R.; Hong, Y. J.; Pillar, R.; Sizgek, E. Sol-Gel Processing by Aging and Pore Creator Addition for Porous Silica Antireflective Coatings. *J. Sol-Gel Sci. Technol* **2002**, *25*, 215–221. DOI: [10.1023/A:1020243527580](https://doi.org/10.1023/A:1020243527580).
- [10] Dou, W.; Niu, Y.; Liu, X.; Xu, Y.; Wen, Z.; Wang, X. Preparation of Single-Layer Antireflective SiO₂ Coating with Broadband Transmittance Using PEG-Modified Sol-Gel Method. *J. Sol-Gel Sci. Technol.* **2013**, *68*, 302–306. DOI: [10.1007/s10971-013-3168-5](https://doi.org/10.1007/s10971-013-3168-5).
- [11] Liu, H.; Wang, P.; Fan, Q.; Luo, J.; Xiao, P.; Jiang, B. $\lambda/4$ - $\lambda/4$ Double-Layer Broadband Antireflective Coatings with Constant High Transmittance. *Coatings* **2022**, *12*, 435. DOI: [10.3390/coatings12040435](https://doi.org/10.3390/coatings12040435).
- [12] Jin, Z.; Deng, Z.; Jia, H.; Yang, C.; Wang, Y.; Wu, H.; Zhu, S.; Yang, X. Preparation and Characterization of Superhydrophilic TiO₂-SiO₂ Films for Double-Layer Broadband Antireflective Coating. *J. Porous Mat.* **2024**, 1–10. DOI: [10.1007/s10934-024-01648-y](https://doi.org/10.1007/s10934-024-01648-y).
- [13] Huang, J. Y.; Wang, Y.; Fei, G. T.; Xu, S. H.; Zeng, Z.; Wang, B. TiO₂/ZnO Double-Layer Broadband Antireflective and down-Shifting Coatings for Solar Applications. *Ceram. Int.* **2023**, *49*, 11091–11100. DOI: [10.1016/j.ceramint.2022.11.305](https://doi.org/10.1016/j.ceramint.2022.11.305).
- [14] Kumar, A.; Nayak, D.; Sahoo, P.; Nandi, B. K.; Saxena, V. K.; Thangavel, R. Fabrication of Porous and Visible Light Active ZnO Nanorods and ZnO@TiO₂ Core-Shell Photocatalysts for Self-Cleaning Applications. *Phys. Chem. Chem. Phys.* **2023**, *25*, 16423–16437. DOI: [10.1039/d3cp01996a](https://doi.org/10.1039/d3cp01996a).

- [15] Koysuren, H. N.; Koysuren, O. Transparent Self-Cleaning Coating Prepared from SiO₂/B₄C and SiO₂/B₄C/TiO₂ for the Solar Cell. *J. Sol-Gel Sci. Technol.* **2024**, *111*, 955–965. DOI: [10.1007/s10971-024-06505-7](https://doi.org/10.1007/s10971-024-06505-7).
- [16] Chandralekha, N. R.; Shanthi, J.; Cathelene Antonette, L.; Anoop, K. K. Improved Efficiency of Solar Cell Using Silane Based SnO₂ Thin Films with Self-Cleaning and Antifogging Properties. *Silicon* **2024**, *16*, 5121–5134. DOI: [10.1007/s12633-024-03047-z](https://doi.org/10.1007/s12633-024-03047-z).
- [17] Rajagopalan, N.; Kiil, S. Self-Sustaining Antifouling Coating for Underwater Solar Cells. *Prog. Org. Coat.* **2024**, *196*, 108754. DOI: [10.1016/j.porgcoat.2024.108754](https://doi.org/10.1016/j.porgcoat.2024.108754).
- [18] Makuła, P.; Pacia, M.; Macyk, W. How to Correctly Determine the Band Gap Energy of Modified Semiconductor Photocatalysts Based on UV–Vis Spectra. *J. Phys. Chem. Lett.* **2018**, *9*, 6814–6817. DOI: [10.1021/acs.jpcllett.8b02892](https://doi.org/10.1021/acs.jpcllett.8b02892).
- [19] Sreemany, M.; Sen, S. A Simple Spectrophotometric Method for Determination of the Optical Constants and Band Gap Energy of Multiple Layer TiO₂ Thin Films. *Mater. Chem. Phys.* **2004**, *83*, 169–177. DOI: [10.1016/j.matchemphys.2003.09.030](https://doi.org/10.1016/j.matchemphys.2003.09.030).
- [20] Wu, J.; Tu, J.; Hu, K.; Xiao, X.; Li, L.; Yu, S.; Xie, Y.; Wu, H.; Yang, Y. Sol–Gel-Derived Bayberry-like SiO₂@TiO₂ Multifunctional Antireflective Coatings for Enhancing Photovoltaic Power Generation. *Colloid Surf. A-Physicochem. Eng. Asp.* **2022**, *654*, 130173. DOI: [10.1016/j.colsurfa.2022.130173](https://doi.org/10.1016/j.colsurfa.2022.130173).
- [21] Krins, N.; Bass, J. D.; Julián-López, B.; Evrar, P.; Boissière, C.; Nicole, L.; Sanchez, C.; Amenitsch, H.; Grosso, D. Mesoporous SiO₂ Thin Films Containing Photoluminescent ZnO Nanoparticles and Simultaneous SAXS/WAXS/Ellipsometry Experiments. *J. Mater. Chem.* **2011**, *21*, 1139–1146. DOI: [10.1039/C0JM02823A](https://doi.org/10.1039/C0JM02823A).
- [22] Huang, J. Y.; Fei, G. T.; Xu, S. H.; Wang, B. ZnO-SiO₂ Composite Coating with anti-Reflection and Photoluminescence Properties for Improving the Solar Cell Efficiency. *Compos. Pt. B-Eng* **2023**, *251*, 110486. DOI: [10.1016/j.compositesb.2022.110486](https://doi.org/10.1016/j.compositesb.2022.110486).
- [23] Aziz, W. J.; Ramizy, A.; Ibrahim, K.; Hassan, Z.; Omar, K. The Effect of anti-Reflection Coating of Porous Silicon on Solar Cells Efficiency. *Optik* **2011**, *122*, 1462–1465. DOI: [10.1016/j.ijleo.2010.08.025](https://doi.org/10.1016/j.ijleo.2010.08.025).
- [24] Javier, G. M.; Dwivedi, P.; Buratti, Y.; Perez-Wurfl, I.; Trupke, T.; Hameiri, Z. Improvements and Gaps in the Empirical Expressions for the Fill Factor of Modern Industrial Solar Cells. *Sol. Energy Mater. Sol. Cells* **2023**, *253*, 112183. DOI: [10.1016/j.solmat.2023.112183](https://doi.org/10.1016/j.solmat.2023.112183).
- [25] Xavier, T. P.; Piraviperumal, M. Self-Cleaning Hydrophobic Coating Composed of Micro/Nano-Imprinted Polydimethylsiloxane with Enhanced Light in-Coupling Capabilities. *ACS Appl. Mater. Interfaces.* **2024**, *16*, 44114–44126. DOI: [10.1021/acsami.4c10614](https://doi.org/10.1021/acsami.4c10614).